Computer Communications 236 (2025) 108122

Contents lists available at ScienceDirect

Computer Communications

journal homepage: www.elsevier.com/locate/comcom

Energy efficient LEO satellite communications: Traffic-aware payload switch-off techniques☆

Vaibhav Kumar Gupta [a,*,1], Hayder Al-Hraishawi [c,2], Eva Lagunas [b], Symeon Chatzinotas [b]

[a] Department of ECE, The LNM Institute of Information Technology, Jaipur, 302031, Rajasthan, India
[b] Interdisciplinary Centre for Security, Reliability and Trust (SnT), University of Luxembourg, 1855, Luxembourg
[c] Department of Electrical Engineering, University of South Florida, Tampa, FL 33620, USA

ARTICLE INFO

Keywords:
Energy efficiency
LEO constellation
Non-terrestrial network
Beam assignment
Successive convex approximation

ABSTRACT

Low Earth orbit (LEO) satellite constellations have a pivotal role in shaping the future of communication networks by providing extensive global coverage. However, ensuring the long-term viability of LEO constellations relies on addressing significant challenges, particularly in the domains of energy efficiency and maximizing the lifespan of satellites. This paper introduces a novel approach that considers user traffic demands to optimize power consumption. By implementing a traffic-aware strategy, redundant satellites can be intelligently switched-off, resulting in significant power savings within the LEO constellation. To accomplish this objective, we formulate the problem of joint satellite beam assignment and beam power allocation as a mixed binary integer optimization problem while carefully considering the constraints imposed by satellite-user visibility and the need to fulfill the data traffic requirements of all ground users. To tackle the formulated problem, we employ a framework called the Difference of Convex Programming and Multiplier Penalty (DCMP) based convexification approach, which ensures convergence to a local optimum. The reformulated convex problem is solved using the low-complexity iterative algorithm, Successive Convex Approximation (SCA). Additionally, we propose a heuristic algorithm based on slant distance, which offers a simplified and efficient solution to the joint problem. To corroborate the effectiveness and validity of the proposed techniques, we assess and compare their performance via simulations, considering practical constellation patterns and realistic user traffic distribution. It has been shown that approximately 43% of the satellite nodes can be switched-off for energy saving, and thus, extending the constellation lifetime and reducing the aggregated interference from multi-beam satellites.

1. Introduction

Low Earth orbit (LEO) satellites offer reduced signal latency, improved coverage, and enhanced capacity comparing to geostationary orbit (GSO) and other non-geostationary orbit (NGSO) satellites [2]. Thus, the number of launched LEO satellites is currently soaring to establish mega-constellations for greater Internet connectivity and global reliable coverage from space [3]. In this direction, the integration of LEO infrastructure with terrestrial networks has attracted significant attention from the telecommunications industry and standardization organizations. Notably, the third-generation partnership project (3GPP) standards group has identified multiple viable pathways to facilitate a wide range of fifth-generation (5G) services and to bridge the digital divide [4]. Specifically, the integration of satellite-based non-terrestrial networks (NTN) with terrestrial communication systems marks a significant transition in research focus and an industry-driven advancement towards the upcoming sixth-generation (6G) wireless networks [5].

However, LEO satellites face stringent power constraints due to their reliance on solar panels and rechargeable batteries that are interchangeably used as energy sources to operate the satellite components [6]. LEO satellites operate with small batteries in order to maintain their compact size, which in turn enables a large number of deployments with a single launch. They also experience shadow periods for a significant portion of their constellation period. Thus,

☆ This work in part was presented at the IEEE Global Communications Conference (Globecom) 2022, Rio de Janeiro, Brazil [1].

This work is financially supported by the Dept. of Telecommunication, Govt. of India under a project, grant reference (TTDF/6G/249), and by the Luxembourg National Research Fund (FNR) under the project MegaLEO (C20/IS/14767486).

* Corresponding author.
E-mail address: vaibhav.gupta@lnmiit.ac.in (V.K. Gupta).

[1] Earlier, Vaibhav Kumar Gupta was with the Interdisciplinary Centre for Security, Reliability and Trust (SnT), University of Luxembourg, 1855 Luxembourg.
[2] Hayder Al-Hraishawi was with the Interdisciplinary Centre for Security, Reliability and Trust (SnT), University of Luxembourg, 1855 Luxembourg.

https://doi.org/10.1016/j.comcom.2025.108122
Received 6 June 2024; Received in revised form 26 October 2024; Accepted 25 February 2025
Available online 12 March 2025

addressing the challenge of reducing energy consumption while continuously ensuring quality-of-service (QoS) remains a critical issue in the context of LEO constellations [7]. Specifically, energy minimization, a crucial aspect in wireless networks [8], is of utmost importance in enhancing the performance of LEO satellite communications. Typically, the electrical power system of a satellite holds significant importance in ensuring mission success. Adequate power provision throughout the satellite's operational lifespan is essential for accomplishing its objectives. However, integrating larger power generation and storage sources, along with power control units, onto a satellite presents daunting challenges. Furthermore, maintaining thermal control in space adds to the complexity of the task. By prioritizing energy efficiency, LEO satellite systems can effectively manage their power consumption, leading to extended operational lifetimes and enhanced system performance [9]. This can also result in advantages such as reduced payload mass, improved launch efficiency, and mitigation of component aging issues, particularly in case of amplifiers where performance degradation occurs monotonically with the time of operation.

The surge in electrical power demand among small satellites has heightened the necessity for on-board power sources with high energy and power densities. This escalation holds particular significance for NASA's proposed future interplanetary missions [10]. Projections indicate that future missions will require power densities ranging between 150 and 250W/kg and specific energies surpassing 250 Wh/kg. Traditionally, small satellite power systems have relied on photovoltaic solar technologies, offering specific power ranging from approximately 20W/kg to 100W/kg. Additionally, these systems often integrate an on-board energy storage device, with advanced lithium-polymer or -ion batteries being the prevalent choice, featuring specific energies between 150 and 250 Wh/kg. Besides, solar power systems in their current state of practice (SOP) exhibit restricted performance capabilities in low irradiance, low temperature, and corrosive environments. Therefore, these existing systems may not adequately meet the demands of future missions, necessitating exploration into alternative efficient power-saving solutions [11].

To foster sustainability in satellite communication systems, it is imperative to devise innovative approaches that focus on minimizing power consumption. This can be achieved through implementing energy-saving mechanisms, utilizing of energy-efficient technologies, and adopting optimized installation practices [12]. Incorporating energy-saving mechanisms, such as sleep modes or dynamic power management enables satellite systems to reduce power usage during periods of low activity. Moreover, maximizing battery lifetime is essential for ensuring long-term reliable operation of LEO satellites [13]. Given the impracticality of battery replacement in space, implementing energy-efficient mechanisms is vital for extending their lifespan. By minimizing electricity consumption, LEO satellites can effectively utilize their limited onboard energy resources and operate reliably over extended periods. This not only enhances the sustainability of satellite communication systems but also reduces the need for costly and challenging battery replacement missions, thereby improving overall operational efficiency.

In the literature, some contributions have studied and developed power control and energy efficiency techniques for LEO satellite transmissions. For example, two optimal power control schemes for LEO satellite constellations integrated with terrestrial networks have been proposed in [14] to maximize delay-limited capacity and minimize outage probability. In [13], the application of Q-learning is explored for optimizing power allocation in satellite-to-ground communications with LEO satellites. In this, the proposed method aims to extend the battery lifetime of LEO satellites by sharing the workload among different satellites. The authors in [15] have developed a communication method to increase the battery lifetime of satellite antennas by controlling transmission power and gain based on the battery's deterioration state. In [16], the optimization of beam assignment and power allocation in a single LEO satellite has been studied for maximizing energy efficiency, considering impairments from Ka-band channels, inter-beam interference, and Doppler effects. Additionally, the utilization of beam hopping techniques can contribute to power savings by dynamically adjusting the beam direction, focusing the satellite transmission power only where it is needed, which has been extensively studied in [17].

Furthermore, LEO satellites traverse the Earth's orbit at significant velocities in comparison to a stationary ground reference point. This inherent motion results in a dynamic ground coverage area, allowing them to cater to diverse geographical regions characterized by varying user concentrations and fluctuating communication requirements. This is particularly relevant in cases of irregular or absent demand, such as in sparsely populated territories [18]. Leveraging this cyclical variation in data needs, developing an adaptive strategy for satellite/beam management that is attuned to traffic patterns can have a twofold advantage: conserving satellite onboard energy and enhancing operational efficiency of the constellation. With the limited resources and a dynamic environment of LEO constellations, the radio resource management system must allow multiple degrees of freedom and adapt to changing conditions. To ensure the effectiveness of the LEO constellation, it is crucial to develop effective radio resource management algorithms that can handle these challenges and enable efficient resource allocation.

To maximize the operational lifespan of LEO satellites and enhance their energy efficiency, researchers have been exploring various techniques. One key approach is to intelligently manage the satellite's communication payload based on the traffic demand it experiences. This involves selectively switching off communication components or modules when the satellite is not actively transmitting data. Within this framework, only a limited number of previous studies have addressed the concept of switching off redundant satellites in order to enhance overall system energy efficiency. As an example, there exists a proposed framework in [19] aimed at minimizing the total count of operational satellite beams necessary to cover all ground-based terminals. Additionally, in [20], simple heuristic algorithms are introduced to aggregate distributed traffic from multiple satellites onto a single satellite, subsequently allowing for the deactivation of unnecessary satellite nodes. Likewise, [21] leveraged geographical discrepancies and weather conditions to strategically power down satellite nodes during periods of reduced traffic, all while ensuring the requisites of connectivity and quality-of-service (QoS). Similarly, [16] delved into the problem of optimizing energy efficiency within a multi-beam single LEO satellite system. Further, the work in [22] has developed an activation strategy for LEO satellite nodes by utilizing the cell-free massive MIMO communication scheme for ameliorating system energy efficiency.

However, the existing works have overlooked crucial factors such as the visibility constraints between the LEO constellation and ground users, as well as the dynamic characteristics of satellite constellations and the fluctuations in user demands. Additionally, the aforementioned techniques have not been analyzed under practical channel models that take into account space-to-Earth propagation effects and the diverse factors contributing to path loss such as atmospheric gasses and the ionospheric and tropospheric effects [23]. Accordingly, our work in this paper is motivated by the identified gaps in existing research and seeks to address them by proposing a novel power allocation strategy for LEO satellites. This strategy takes into consideration these crucial factors, i.e., the visibility constraints, LEO flight dynamics, and user demand variations, along with utilizing the developed LEO channel models within the 3GPP standardization efforts to introduce New Radio (NR) based NTN solutions [24]. By incorporating these factors and considering the inherited system configurations, our proposed strategy aims to provide a practical and effective solution to optimize power consumption in LEO satellite communication systems. In summary, the main contributions of this paper can be outlined as follows:

- Develop a novel approach for beam assignment, active beam power allocation, and satellite switch-off technique based on the dynamic patterns of LEO satellite constellations, practical 3GPP channel models, and realistic user traffic demands.
- Formulate a joint beam assignment and power allocation problem as an optimization problem with the objective of minimizing the total power consumption of the LEO constellation while ensuring full satisfaction of the ground user demands.
- Employ a Difference of Convex Programming and Multiplier Penalty (DCMP) framework to convexify the formulated non-convex mixed-integer problem. This approach can effectively solve the optimization problem and find a feasible solution by transforming the problem into a convex form.
- Develop an iterative algorithm based on successive convex approximation (SCA) to solve the formulated problem. This algorithm guarantees convergence to a local optimum solution while keeping the computational complexity low.
- Propose a low-complexity heuristic algorithm based on the user-satellite slant distance to solve the formulated joint problem. This algorithm offers a practical and efficient solution approach with much reduced computational complexity.
- The performance of the proposed techniques is investigated herein in terms of the number of satellite nodes/beams that can be switched-off, total power consumption and the energy efficiency of the system. Simulation results including performance comparisons are provided to demonstrate the validity and gain of the proposed methods over the solution provided in [1].

The paper is organized as follows. In Section 2 we describe the system and channel model. Section 3 discusses optimization problem formulation and then, its convexification and the SCA based algorithm is proposed in Section 4.1. A low complexity heuristic algorithm is proposed in Section 4.2. The time complexity of the proposed algorithms are provided in Section 5. Section 6 introduces the numerical results and finally Section 7 provides concluding remarks.

2. System and channel model

We consider a multi-beam LEO satellite constellation consisting of N LEO satellites to serve M ground users. Denoting the sets of LEO satellite nodes and ground users as $\mathcal{N} = \{1, \ldots, N\}$ and $\mathcal{M} = \{1, \ldots, M\}$ respectively, we define N_B as the upper limit for the number of users that a satellite can simultaneously accommodate. This value also corresponds to the maximum number of beams per satellite. Namely, each user is assumed to be served by a single pencil-like beam as depicted in Fig. 1. We consider the Earth-moving cell coverage architecture that is a dynamic system where users within the coverage area of each satellite continuously change over time. This architecture offers the advantage of reduced satellite costs since there is no need for a satellite beam steering mechanism. Note that this architecture option has already been specified by the 3GPP standardization body as part of the integration solutions for 5G-NTN [25]. Consequently, a user can be served by multiple satellites at different times depending on satellite-user visibility constraint. This implies that users are multiplexed using Time Division Multiple Access (TDMA), enabling simultaneous service for multiple users by a specific satellite. Additionally, the maximum number of users that can be served in a single TDMA slot is determined by the number of beams that can be generated concurrently.

In this system, LEO satellites are equipped active antenna arrays, while user terminals are equipped with tracking antennas. Consequently, we introduce the visibility matrix $\mathbf{V}(t) = \{v_{n,m} | n \in \mathcal{N}, m \in \mathcal{M}\}$, which signifies the feasible set of satellites that could potentially serve the mth user at a given time instant t. In particular, $v_{n,m} \in \{0, 1\}$ acts as a binary visibility indicator, where $v_{n,m} = 1$ signifies the availability of the nth satellite to serve the mth user; else, $v_{n,m} = 0$. Notably, users typically exhibit heterogeneous spatio-temporal traffic requirements

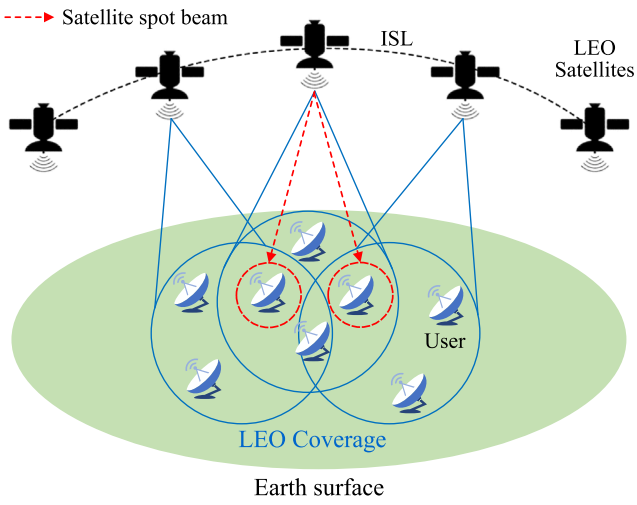

Fig. 1. An illustrative depiction of the coverage provided by a multi-beam LEO satellite constellation, along with the distribution of ground users across the Earth's surface.

across the globe. To accommodate this varying distribution of user demands within the system, $D_m(t)$ represents the data traffic demand in bits per second (bps) of the mth user at time instance t, and this demand should be satisfied by a satellite that is visible to the user.

2.1. Channel model

The link quality from LEO satellite constellation to the users undergo alterations due to a sequence of attenuation phenomena. In this context, Release-15 of the 3GPP introduces a range of NTN channel models designed for diverse scenarios, including those corresponding to our system models. Therefore, it is more pragmatic to thoroughly examine and assess the proposed system model by integrating the established 3GPP NTN channel model. As a result, signal-to-noise ratio (SNR) of the link from the nth satellite to the mth user can be represented in decibels (dB) using the following expression [26]:

$$SNR_{n,m} = G_t + G_r + P_{n,m} - PL_m^n - P_n \tag{1}$$

where $G_t, G_r, P_{n,m}, PL_m^n$ and P_n are all measured in dB and stand for, respectively, the satellite transmitting antenna gain, user receiver antenna gain, transmit power from the nth satellite to the mth user, the total path loss and thermal noise power at the mth user. In a linear scale, the SNR is expressed as:

$$\gamma_{n,m} = \frac{g_t \; g_r \; p_{n,m}}{pl_m^n \; p_n} \tag{2}$$

Here, the various terms represent the respective linear scale equivalents of the terms which are outlined in (1).

Next, the primary contributors to the total path loss are the fundamental path loss along the link between the nth satellite and the mth user, $PL_b(n, m)$, the attenuation due to atmospheric gasses, PL_g, and the attenuation due to either ionospheric or tropospheric scintillation, PL_s. These factors fluctuate with the satellite's movement, and variation in path losses will directly impact the capacity of the satellite service link. By integrating the 3GPP NTN channel model, the cumulative path loss encountered along the communication link between the nth satellite and the mth user, denoted as PL_m^n, can be mathematically formulated as [26]

$$PL_m^n = PL_b(n, m) + PL_g + PL_s. \tag{3}$$

Each of the elements contributing to path loss in (3) is quantified in dB. More specifically, the fundamental path loss model $PL_b(n, m)$ encapsulates the effects of signal propagation through free space, clutter

loss, and shadow fading. Specifically, the fundamental path loss (PL_b) expressed in decibels (dB) is formulated as follows:

$$PL_b(n,m) = PL_{FS}(d_s, f_c) + SF + CL(\alpha, f_c). \tag{4}$$

where, PL_{FS}, SF and $CL(\alpha, f_c)$ are free space path loss, loss due to shadow fading and clutter loss, respectively. The logarithmic representation of the free space path loss (PL_{FS}) in dB, considering a given distance d_s (also known as slant range between the nth satellite and the mth user) in meter along with frequency f_c in GHz can be computed as

$$PL_{FS}(d_s, f_c) = 32.45 + 20\log_{10}(f_c) + 20\log_{10}(d_s). \tag{5}$$

A mathematical model employing log-normal distribution as $\mathcal{LN}(0, \sigma^2_{SF})$ with zero-mean and σ_{SF} standard deviation is used to characterize shadow fading (SF). Clutter loss (CL) pertains to the reduction in signal strength due to the presence of nearby structures and objects within the Earth's surroundings. This phenomenon is influenced by factors such as the carrier frequency f_c, the angle of the elevation angle (α), and the environment. It is important to note that when a user has Line-of-Sight (LOS) connection, the clutter loss becomes negligible, effectively being considered as 0 dB in the fundamental path loss model. From Tables 6.6.2-1 and 6.6.2-3 in the 3GPP Release-15, the values for σ^2_{SF} and CL can be derived.

Furthermore, it is plausible to assume that the channel realizations between the satellite and various users are uncorrelated since the users are physically separated by a few wavelengths [27]. Additionally, within such systems, a 4-color reuse frequency scheme can be taken into account, permitting frequency reuse while keeping interference at a minimum level among adjacent beams [28,29].

3. Problem formulation

The main objective of this study is to minimize the overall power consumption of the LEO satellite constellation while meeting the user demands within a specified time horizon, denoted as T, which represents the constellation periodicity. Specifically, our primary focus is to reduce the number of active satellites in the constellation.[3] It should be noted that complete satellite shutdown is not feasible as certain control components need to remain operational. Therefore, our proposed approach primarily concentrates on deactivating the communications payload to achieve power savings. In this framework, we consider the instantaneous transition of satellite states between on-off and off-on operation modes, which is assumed to have negligible energy consumption and is achieved through telemetry, tracking, and control (TT&C) commands. To this end, a binary assignment variable is defined to indicate whether a satellite is active or switched-off as follows

$$Y_n = \begin{cases} 1, & \text{satellite } n \text{ is active} \\ 0, & \text{satellite } n \text{ is switched-off.} \end{cases} \tag{6}$$

Similarly, we introduce a binary association variable that indicates whether a satellite beam is serving a user. This variable is defined as follows:

$$X_{n,m} = \begin{cases} 1, & \text{a beam of satellite } n \text{ is assigned to serve user } m \\ 0, & \text{otherwise.} \end{cases} \tag{7}$$

In principle, the aggregate transmit power of each individual satellite must adhere to its designated power budget. To be more precise, the total transmit power budget of each satellite is represented as P_T, which is the summation of satellite transmit power to the served users plus the fixed on-board circuit power consumption when the satellite communication payload is switched-on. Within this context, $P_{n,m}(t)$ denotes the transmit power of the nth satellite to the mth user at the time slot t, whereas P_c stands for the fixed circuit power consumption. Additionally, it is presumed that each active beam has the same maximum transmit power and bandwidth similar to the works in [16,30], which are designated as P_b and W, respectively. Accordingly, the maximum beam transmit power (P_b) can be computed as

$$P_b = \frac{P_T - P_c}{N_B}. \tag{8}$$

Thus, a joint optimization problem of satellite beam assignment and minimizing the total power consumption of LEO satellite constellation can be formulated as follows:

$$\begin{aligned}
&\underset{\forall P_{n,m}, \forall X_{n,m}, \forall Y_n}{\text{minimize}} \quad \sum_{t=1}^{T}\sum_{n=1}^{N}\sum_{m=1}^{M} P_{n,m}(t) + \sum_{t=1}^{T}\sum_{n=1}^{N} P_c\, Y_n(t) \\
&\text{subject to C1:} \quad 0 \le P_{n,m}(t) \le P_b, \quad \forall n, \forall m \\
&\qquad \text{C2:} \quad \sum_{n\in\mathcal{N}} X_{n,m}(t) \le 1, \quad \forall m, \\
&\qquad \text{C3:} \quad \sum_{n\in\mathcal{N}} X_{n,m}(t) \le D_m(t), \quad \forall m \\
&\qquad \text{C4:} \quad \sum_{m=1}^{M} X_{n,m}(t) \le N_B, \quad \forall n \\
&\qquad \text{C5:} \quad \sum_{m=1}^{M} X_{n,m}(t) \le M_0 Y_n(t), \quad \forall n \\
&\qquad \text{C6:} \quad X_{n,m}(t) \le \upsilon_{n,m}(t), \ \forall n, \forall m, \forall t \\
&\qquad \text{C7:} \quad \sum_{n\in\mathcal{N}} W \log_2\left(1 + X_{n,m}(t)\gamma_{n,m}(t)\right) \ge D_m(t), \qquad \forall m, \forall t \\
&\qquad \text{C8:} \quad X_{n,m}, Y_n \in \{0,1\}.
\end{aligned} \tag{9}$$

The initial term within the objective function in (9) accounts for the total transmit power of the satellite constellation to meet user demands, while the subsequent term corresponds to the constant power consumption of the onboard circuits when the satellite is active. Constraint C1 firmly establishes that the satellite transmit power to a user must not exceed the specified maximum beam power P_b. Constraints C2 and C3 dictate that each user can only be served by one satellite at a time, and a user can only be served if it has some non-zero demand, respectively. To ensure that no satellite overextends its capacity, Constraint C4 is implemented, limiting each satellite to serve no more than N_B users concurrently. In Constraint C5, the introduction of a significantly large value M_0 signifies that a satellite is activated when it serves at least one user within a given time slot. Constraint C6 is responsible for ensuring that a satellite exclusively serves users within its coverage area, thereby remaining visible to them. Constraint C7 is designed to satisfy users' traffic requirements at every time instance. Lastly, Constraint C8 enforces the binary restriction on the assignment variables $X_{n,m}$, and Y_n.

In previous research, the problem at hand was addressed in our recent publication in [1]. Although the proposed solution in [1] is valid and provides an optimal solution in high SNR regime, it falls short when it comes to users with low or medium demands. The total satellite transmit power obtained from the previous solution is suboptimal and relatively high in these scenarios. Building upon this motivation, this work aims to develop a more comprehensive and optimal solution to tackle this problem.

4. Proposed solutions

The optimization problem formulated in the previous section exhibits a combinatorial mixed integer nature primarily because of the presence of binary assignment variables. Additionally, constraint C7 transforms the problem into one that is both non-linear and non-convex in nature. In this section, two effective methods for dealing with the non tractability of problem (9) are presented.

[3] From a practical standpoint, it is more preferable to deactivate specific satellites rather than keeping many satellites operating at low power levels.

4.1. SCA-based proposed solution

To ensure practicality and ease of handling, we can introduce reasonable and pragmatic assumptions that simplify the complexity of the aforementioned optimization problem. This will allow us to propose a viable solution that can be effectively implemented centrally at the satellite gateway. Specifically, the non-convexity of formulated problem in (9) is addressed in this section via a suboptimal algorithm that consists of three basic phases.

First, the time horizon T is segmented into equidistant time slots,[4] allowing us to address the optimization problem individually within each time slot. By focusing on the optimization problem within each time slot, it is plausible to exclude the time index (t) and sum over time horizon T. In second phase, to obtain a local optimal solution of the optimization problem in (9), we use a combination of difference of convex (DC) programming and multiplier penalty (MP) method [31], [32]. Then, finally we employ SCA method to obtain locally optimal solution.

4.1.1. DCMP method

To tackle the binary integer variable issue in C8, we use a combination of difference of convex programming and multiplier penalty (DCMP) method. For this purpose, let $\mathbf{P}$, $\mathbf{X}$ and $\mathbf{Y}$ be the collection of optimization variables $P_{n,m}, X_{n,m}, \forall n, m$ and $Y_n, \forall n$, respectively. The binary integer constraints for $X_{n,m}$ and Y_n in C8 are rewritten in the form of DC functions as follows:

$$\begin{aligned}
&\text{C8a:}\quad 0 \le X_{n,m} \le 1, \forall m, n\\
&\text{C8b:}\quad G_x(\mathbf{X}) - F_x(\mathbf{X}) \le 0,\\
&\text{C8c:}\quad 0 \le Y_n \le 1, \forall n\\
&\text{C8d:}\quad G_y(\mathbf{Y}) - F_y(\mathbf{Y}) \le 0,
\end{aligned} \tag{10}$$

where

$$G_x(\mathbf{X}) = \sum_{n=1}^{N}\sum_{m=1}^{M} X_{n,m} \text{ and, } F_x(\mathbf{X}) = \sum_{n=1}^{N}\sum_{m=1}^{M}(X_{n,m})^2$$

$$G_y(\mathbf{Y}) = \sum_{n=1}^{N} Y_n \text{ and, } F_y(\mathbf{Y}) = \sum_{n=1}^{N}(Y_n)^2.$$

The binary assignment variables in C8 are now equivalently transformed in continuous form as in (10). However, since C8b and C8d are reverse convex constraints, they are still not convex. To circumvent this challenge, we apply MP method in which the penalty is introduced in the objective function as a Lagrange multiplier of the reverse convex constraint. Now, we introduce the subsequent theorem.

Theorem 1. *Problem (9) is equivalent to the following problem for sufficiently large constants α_1 and α_2:*

$$\begin{aligned}
&\underset{\mathbf{P},\mathbf{X},\mathbf{Y}}{\text{minimize}} \quad \Phi(\mathbf{P},\mathbf{X},\mathbf{Y}) = \textstyle\sum_{n=1}^{N}\sum_{m=1}^{M} P_{n,m} + \sum_{n=1}^{N} P_c\, Y_n + \eta(\mathbf{X},\mathbf{Y})\\
&\text{subject to} \qquad\qquad C1\text{-}\ C7, C8a,\ C8c,
\end{aligned} \tag{11}$$

where

$$\eta(\mathbf{X},\mathbf{Y}) = \alpha_1(G_x(\mathbf{X}) - F_x(\mathbf{X})) + \alpha_2(G_y(\mathbf{Y}) - F_y(\mathbf{Y})). \tag{12}$$

Proof. Please refer to Appendix. □

For any $X_{n,m}$ and Y_n that is not equal to 0 or 1, the constants α_1, and α_2 serve as penalty factors to penalize the objective function. Now, the non convexity of the problem (11) is only due to non convex objective function. In the next section, we implement SCA method to approximate the optimization problem (11) by a convex problem and, then an iterative low complexity algorithm is proposed to effectively solve the convex problem.

[4] The duration of a time slot is selected such that the satellite constellation, downlink link budget, and the visibility matrix are changed with every time slot.

Algorithm 1 Successive Convex Approximation Based Algorithm

Input: Visibility matrix $\mathbf{V}$, set maximum number of iterations L, iteration index $l = 1$, penalty factors $\alpha_1 >> 1$ and $\alpha_2 >> 1$, initial feasible points $\mathbf{P}^{(1)}, \mathbf{X}^{(1)}$, and $\mathbf{Y}^{(1)}$.
Output: $\mathbf{P}^*, \mathbf{X}^*, \mathbf{Y}^*$

1: **for** $l = 1, \ldots, L$ **do**
2: Solve convex problem (17) for given $\mathbf{P}^{(l)}, \mathbf{X}^{(l)}$, and $\mathbf{Y}^{(l)}$.
3: Set $l = l + 1$ and update $\mathbf{P}^{(l+1)} = \mathbf{P}^{(l)}, \mathbf{X}^{(l+1)} = \mathbf{X}^{(l)}$, and $\mathbf{Y}^{(l+1)} = \mathbf{Y}^{(l)}$, and $\Phi_l = \Phi(\mathbf{P}^{(l)}, \mathbf{X}^{(l)}, \mathbf{Y}^{(l)})$.
4: **end for**
5: $\mathbf{P}^* = \mathbf{P}^{(L)}, \mathbf{X}^* = \mathbf{X}^{(L)}$, and $\mathbf{Y}^* = \mathbf{Y}^{(L)}$.
6: **return** $\mathbf{P}^*, \mathbf{X}^*, \mathbf{Y}^*$

4.1.2. SCA method

Due to the fact that its objective function can be expressed as the difference of two convex functions, the optimization problem (11) falls into the category of DC programming problems. Therefore, we use the Taylor series approximation to address the non-convexity of problem (11) by linearizing the non-convex part of the objective function. The following first order approximation inequality holds for any feasible points $\mathbf{X}^{(l)}$ and $\mathbf{Y}^{(l)}$, where the superscript l stands for the SCA iteration index, because F_x and F_y are differentiable convex functions:

$$F_x(\mathbf{X}) \ge \hat{F}_x(\mathbf{X}) = F_x(\mathbf{X}^{(l)}) + \nabla_{\mathbf{X}} F_x(\mathbf{X}^{(l)})^T(\mathbf{X} - \mathbf{X}^{(l)}) \tag{13}$$

$$F_y(\mathbf{Y}) \ge \hat{F}_y(\mathbf{Y}) = F_y(\mathbf{Y}^{(l)}) + \nabla_{\mathbf{Y}} F_y(\mathbf{Y}^{(l)})^T(\mathbf{Y} - \mathbf{Y}^{(l)}). \tag{14}$$

$\hat{F}_x(\mathbf{X})$ and $\hat{F}_y(\mathbf{Y})$ in (13) and (14), where $\nabla_{\mathbf{X}} F_x(\mathbf{X}^{(l)})$ and $\nabla_{\mathbf{Y}} F_y(\mathbf{Y}^{(l)})$ are the gradients of $F_x(\mathbf{X})$ and $F_y(\mathbf{Y})$, respectively, are affine functions that describe the global underestimate of $F_x(\mathbf{X})$ and $F_y(\mathbf{Y})$, respectively. Next, the second term in the definitions of $\hat{F}_x(\mathbf{X})$ and $\hat{F}_y(\mathbf{Y})$ are given by following expressions:

$$\nabla_{\mathbf{X}} F_x(\mathbf{X}^{(l)})^T(\mathbf{X} - \mathbf{X}^{(l)}) = \sum_{n=1}^{N}\sum_{m=1}^{M} 2X_{n,m}^{(l)}(X_{n,m} - X_{n,m}^{(l)}) \tag{15}$$

$$\nabla_{\mathbf{Y}} F_y(\mathbf{Y}^{(l)})^T(\mathbf{Y} - \mathbf{Y}^{(l)}) = \sum_{n=1}^{N} 2Y_n^{(l)}(Y_n - Y_n^{(l)}) \tag{16}$$

By substituting (13) and (14), the optimization problem (11) is reformulated as the following convex optimization problem:

$$\begin{aligned}
&\underset{\mathbf{P},\mathbf{X},\mathbf{Y}}{\text{minimize}} \quad \Phi(\mathbf{P},\mathbf{X},\mathbf{Y}) = \textstyle\sum_{n=1}^{N}\sum_{m=1}^{M} P_{n,m} + \sum_{n=1}^{N} P_c\, Y_n + \hat{\eta}(\mathbf{X},\mathbf{X}^{(l)},\mathbf{Y},\mathbf{Y}^{(l)})\\
&\text{subject to} \qquad\qquad C1 - C7, C8a,\ C8c,
\end{aligned} \tag{17}$$

where $\hat{\eta}(\mathbf{X},\mathbf{X}^{(l)},\mathbf{Y},\mathbf{Y}^{(l)}) = \alpha_1(G_x(\mathbf{X}) - \hat{F}_x(\mathbf{X})) + \alpha_2(G_y(\mathbf{Y}) - \hat{F}_y(\mathbf{Y}))$. Since the objective function is convex and all the constraints are also convex, the optimization problem (17) is convex and can be solved efficiently by using well-known optimization tools such as CVX, a Matlab software for disciplined convex programming [33]. The key steps for solving problem (11) iteratively are outlined in Algorithm 1, where the result of problem (17) in iteration l serves as the starting point for iteration $(l+1)$. Algorithm 1 iteratively solves problem (17), resulting in a series of improved viable solutions, *i.e.,* the solution of each iteration is a feasible solution, for sufficiently large number of iterations, L. Since we minimize the value Φ_l at each iteration, Algorithm 1 generates a nonincreasing sequence $\{\Phi_l\}_{l\ge 0}$ and converge to a finite value C ($\lim_{l\to\infty}\Phi_l = C > -\infty$). Subsequently, under the assumption of appropriate constraint qualifications, it follows that $C = \lim_{l\to\infty}\Phi_l = \Phi(\hat{\mathbf{P}},\hat{\mathbf{X}},\hat{\mathbf{Y}})$ for some stationary point $(\hat{\mathbf{P}},\hat{\mathbf{X}},\hat{\mathbf{Y}})$ of problem (11) or problem (9). Therefore, Algorithm 1 converges to a local optimum point of problem (11) or, alternatively, problem (9) in polynomial time [34].

4.2. Heuristic algorithm

This section introduces a heuristic algorithm to solve the joint beam assignment and power minimization problem formulated in Section 3. The intractability of the formulated joint problem is mainly due to binary association variables, *i.e.,* **X** and **Y**. To start, we decompose the joint problem into two distinct sub-problems: (1) the user-satellite association problem, and (2) the power allocation problem. This division allows us to address each sub-problem independently and devise efficient solutions for both aspects of the larger problem. To solve the first subproblem, we propose a low complexity user-satellite slant distance based heuristic algorithm as detailed in Algorithm 2 and once the association variables are known, the power allocation can be obtained by solving problem (9) with known association variables **X** and **Y** from Algorithm 2 .

Algorithm 2 presents a streamlined and less complex approach for associating users with LEO satellites in each time slot. To expedite the association process, Algorithm 2 utilizes the slant distance between users and satellites. Specifically, this algorithm associates each user with the nearest visible LEO satellite, enabling a faster and more efficient association process. Fundamentally, the core concept of the association algorithm is to ensure that each user is served by the nearest visible satellite. This approach aims to optimize both the channel quality for the user and minimize the transmit power required by the satellite. The inputs to the algorithms are user set $\mathcal{N}$, LEO satellite nodes $\mathcal{M}$, slant distance of all the users from all LEO satellites, satellite visibility matrix **V** and maximum number of beams per satellite N_B. To begin with, the proposed association algorithm arrange the user set in the increasing order of the number of visible satellites. This is because if there is only one satellite visible to user, then associate the user with the visible satellite and remove the user from the set of users. Now, if there are multiple satellites visible to a user, then choose the nearest visible satellite and associate the user with the satellite if it is serving fewer than N_B users; otherwise select the second nearest satellite and so on. Finally, the algorithm output is a list of user satellite association, i.e., association matrix **X** whose element $X_{n,m}$ equals to 1 if satellite n and user m is there in the output association list.

Next, using the outputs obtained from Algorithm 2, the association binary variables **X** and **Y**, problem (9) can be translated to the following convex optimization problem:

$$\begin{aligned} \underset{\forall P_{n,m}}{\text{minimize}} \quad & \sum_{t=1}^{T}\sum_{n=1}^{N}\sum_{m=1}^{M} P_{n,m}(t) + \sum_{t=1}^{T}\sum_{n=1}^{N} P_c\, Y_n(t) \\ \text{subject to} \quad & \text{C1, C7.} \end{aligned} \tag{18}$$

Problem (18) can be easily solved using standard optimization tools such as CVX [33]. Finally, the solution of problem (18) is an approximate and efficient solution to the original problem (9).

5. Complexity analysis

In this section, we evaluate the computational complexity of the proposed schemes, aiming to provide insights into their efficiency and feasibility in practical implementations.

5.0.1. SCA based algorithm (Algorithm 1)

Problem (17) is a non linear convex problem with $N(1 + 2M)$ number of variables in each time slot. Therefore, this problem can be solved in polynomial time with the complexity of $O([N(1+2M)]^3)$ [35]. Then, the complexity of SCA-based Algorithm 1 can be estimated as $O([N(1+2M)]^3 \times L)$, where L denotes the number of iterations required to converge.

5.0.2. Heuristic algorithm

The proposed heuristic algorithm works in two phases: (1) User satellite association phase (2) satellite beam power allocation phase. The time complexity of Algorithm 2 which provides user satellite association is $O([N(logN + M)])$ and then the complexity of power allocation phase is $O(N)$. Therefore, the time complexity of heuristic algorithm to solve problem (9) is $O([N(logN + M + 1)])$.

Clearly, the proposed heuristic algorithm has lower complexity than the SCA based algorithm as the latter grows exponentially with the number of users.

Algorithm 2 Slant Distance Based User and LEO Satellite Association

Input: Set of Users: $\mathcal{N}$
Set of LEO satellite nodes: $\mathcal{M}$
Maximum number of beams per satellite: N_B
Visibility Matrix: **V**
Slant distance matrix
Onput: User-satellite association matrix: **X**

```
associations ← []
users_sorted ← Sort users in 𝒩 in increasing order of number of visible satellites
while users_sorted is not empty do
  user ← Remove the first element from users_sorted
  visible_satellites ← V[user]
  if |visible_satellites| = 1 then
    satellite ← Remove the only element from visible_satellites
    Append (user, satellite) to associations
    Remove user from users
  else
    Sort visible_satellites based on user_satellite_slant_distance[user][satellite]
    for each satellite in visible_satellites do
      if |associations| < N_B then
        Append (user, satellite) to associations
        Remove user from users
        break
      end if
    end for
  end if
end while
return associations
```

6. Numerical results

In this section, we evaluate the effectiveness of the proposed satellite switch-off techniques within LEO constellations through a series of simulations. The simulation framework involves a LEO broadband constellation designed according to the Walker star systematic pattern [36]. The spatial arrangement of all LEO satellites within the system is established by the parameters outlined in [37]. Concretely, the Earth's surface is depicted as a planisphere region with longitudes spanning from −180° to 180°° and latitudes ranging from −90° to 90°, as depicted in Fig. 2 and elaborated upon in [38]. The left hemisphere of the planisphere, consisting of longitudes from −180° and 0°, is covered by the ascending satellites traveling from South to North. Conversely, the right hemisphere, consisting of longitudes from 0° and 180°, is covered by descending satellites moving from North to South. Consequently, each satellite's orbital plane is divided into two equal halves, with one situated in the left planisphere and the other in the right planisphere.

Within this configuration, the LEO constellation comprises 140 satellites, evenly distributed across 7 circular orbital planes. Each orbital plane is inclined at 98.6°, ensuring comprehensive coverage of both poles. The orbital period of every satellite is set at 120 min [37, 39]. Additionally, the ith orbital plane's longitude and altitude are set to $180(i-1)/7$ degrees and $600+10(i-1)$ Km, respectively. To calculate visibility between a satellite and a user, we employ Earth-centered,

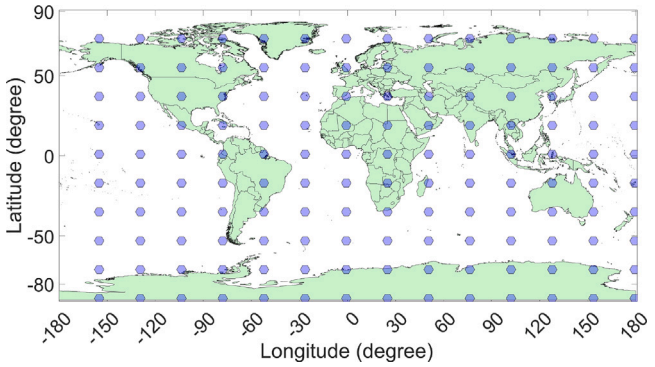

Fig. 2. A schematic diagram of the LEO constellation that includes 140 LEO satellites (represented as blue hexagons) distributed over the Earth surface.

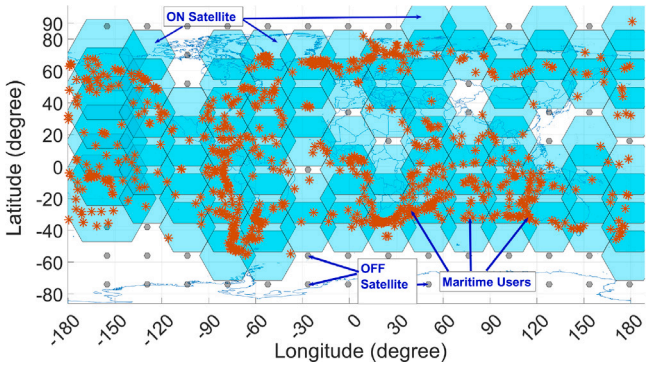

Fig. 3. An illustrative depiction of the constellation coverage is presented, showcasing the association of the active satellites and users as established by the proposed solution to satisfy the requirements of maritime users distributed across the Earth's surface.

Table 1
Simulation parameters [37].

Parameter	Value
Constellation type	Walker Star
Number of LEO satellites	140
Number of orbital planes	7
Altitude of orbital plane $i \in \{1, \ldots, 7\}$	$600 + 10(i-1)$ Km
Orbital period T	120 min
Time slot duration	5 min
Orbit inclination	98.6^o
Max number of beams per satellite N_B	30
Bandwidth W	200 MHz
Downlink carrier frequency f_c	20 GHz
Satellite transmission power P_T	300 Watt
Fixed circuit power P_c	10 Watt [16]
Satellite antenna gain G_t	38.5 dBi
User antenna gain G_r	39.7 dBi
Atmospheric loss	0.3 dB
Scintillation loss	0.5 dB
Noise figure	1.2 dB
Noise temperature	354 K
Penalty factors α_1, α_2	200
Max. Number of SCA iterations L	5

Earth-fixed (ECEF) coordinates for the satellite and user. Generally, a satellite is considered visible to a ground user when the elevation angle (ϵ) surpasses a predetermined minimum threshold. Within this context, ϵ_{min} is configured to be 10° in this study. The slant range d_s from a ground based user to a satellite can be determined as follows [36]:

$$d_s = R_e \left[\sqrt{\left(\frac{H + R_e}{R_e} \right)^2 - \cos^2(\epsilon)} - \sin(\epsilon) \right]. \tag{19}$$

Herein R_e represents the radius of the Earth, while H is the altitude of the satellite orbital plane. To effectively accommodate the relative motion between the satellite constellation and user terminals, a time horizon equivalent to the satellite's orbital period is adopted. This timeframe is subsequently divided into discrete time slots, each lasting 5 min. The positions of all satellite nodes within the constellation are then calculated or updated, and these changes are reflected in the visibility matrix for successive time slots. As for the demand and distribution of users, realistic user locations are derived from a maritime dataset [40], specifically related to cruise ships equipped with broadband connectivity from satellites during the day 30th June 2021. Moreover, key simulation parameters are concisely outlined in Table 1.

Fig. 3 depicts a snapshot of the constellation's coverage, indicating the active satellite distribution derived from the proposed method. Additionally, the spatial distribution of users is represented within a specific time slot. Notably, the coverage region of currently active satellites, serving users, is highlighted in a light green shade, while the non-active satellites are represented by smaller gray hexagons to illustrate their inactive state. The evident observation is that a subset of satellite nodes can be activated to promptly meet the immediate demands of all users, allowing the deactivation of the remaining satellite nodes to conserve energy resources effectively.

Now, we explain the two types of experiment scenarios considered herein, *i.e.,* Scenario-1 and Scenario-2, to run the numerical simulations. In Scenario-1, we maintain a constant number of 200 users in the system and vary their demands to create distinct cases representing high, medium, and low user demand levels. Conversely, in Scenario-2, we set the number of users in the system at 200, 100, and 50,[5] respectively, to encompass high, medium, and low average system demand cases,[6] and the user demands are randomly generated using uniform distributions in each of the three cases [41–43]. The numerical results for the proposed algorithms in terms of downlink transmit power and energy efficiency under Scenario-1 and Scenario-2 are detailed in rest of this section.

6.1. Downlink transmit power

To begin, we conduct a performance comparison of the two algorithms proposed in this paper (*i.e., SCA-based algorithm and heuristic algorithm*), alongside the solution presented in [1], in terms of the satellite transmit power required to meet all user demands. This comprehensive set of experiments is carried out for Scenario-1, enabling us to evaluate the performance of the proposed techniques across various user demand scenarios. Specifically, for the sake of completeness, Fig. 4 depicts the convergence of the proposed SCA Algorithm 1 where the evolution in terms of transmit power (dBW) is shown with respect to iterations for low, medium, and high user demand. It can be observed that Algorithm 1 converges after 5–6 iterations, where transmit power decreases before saturating at a constant value. Furthermore, the results depicted in Figs. 5, 6, and 7 confirm that the two algorithms proposed in this work exhibit superior performance compared to the solution

[5] These two scenarios serve as an abstraction to verify the mathematical framework of our proposed model. The framework is indeed capable of being extended to accommodate a larger number of users. Our primary goal in this phase of the study is to establish the foundational principles of our approach before scaling it to more complex scenarios. We recognize that real-world applications may involve a significantly higher user density, and future work will explore these larger-scale implementations.

[6] For illustration purpose, we selected one business line of LEO satellites which is communications on the move. The annual traffic for LEO satellites, as presented in [21], can be broadly classified into three levels. Additionally, we would like to clarify that the three levels of user demand in our simulations are designed to capture the different types of data rate demands that broadly represent the varying requirements of diverse user applications.

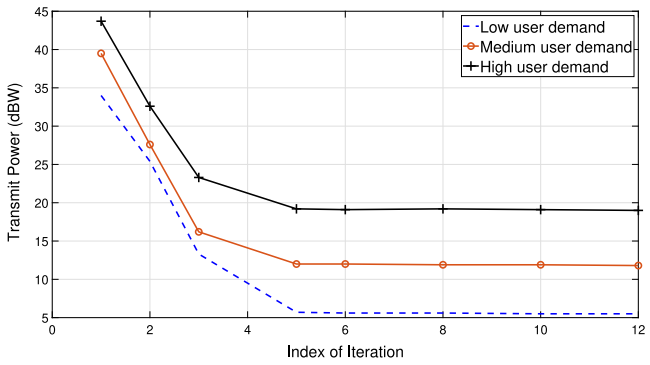

Fig. 4. Convergence of the proposed SCA based Algorithm 1.

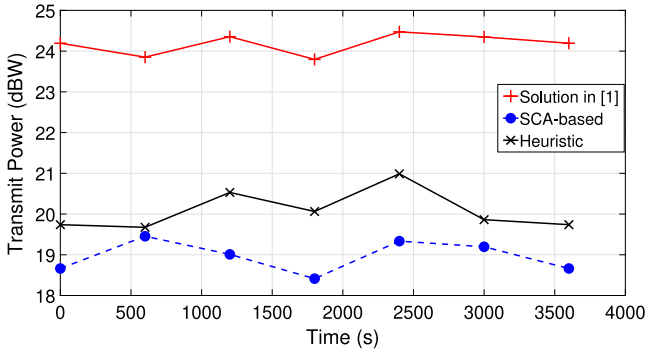

Fig. 5. A comparison of the proposed SCA and heuristic algorithms with the solution proposed in [1], showcasing the satellite transmit power variation over an orbital period for the case of **high** user demand.

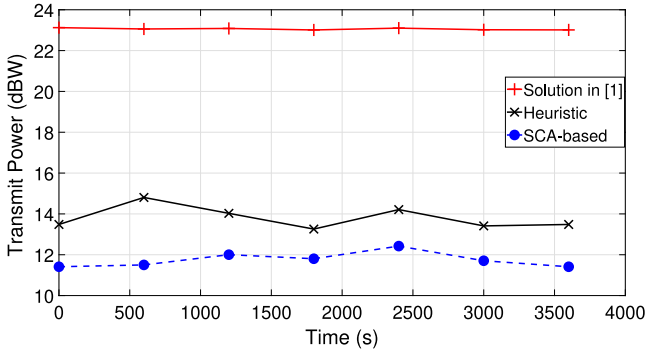

Fig. 6. A comparison of the proposed SCA and heuristic algorithms with the solution proposed in [1] in terms of the satellite transmit power over an orbital period for the case of **medium** user demand.

presented in [1] across high, medium, and low demand cases. Notably, there is a substantial performance gap between the solution in [1] and the proposed algorithms in both the medium and low demand cases. This discrepancy arises from the fact that even for low and medium user demands, the satellite transmit power required to meet these demands cannot be reduced below 1 unit. Hence, it can be observed that the transmit power obtained from the solution proposed in [1] remains relatively constant when the user demands are below a certain threshold value.

Since the solution in [1] underperforms among the evaluated methods, we will next focus exclusively on the performance evaluation of the two proposed algorithms for the considered two scenarios. Particularly, Fig. 8 shows the variation of satellite transmit power over an orbital period for both the SCA-based and heuristic algorithms with

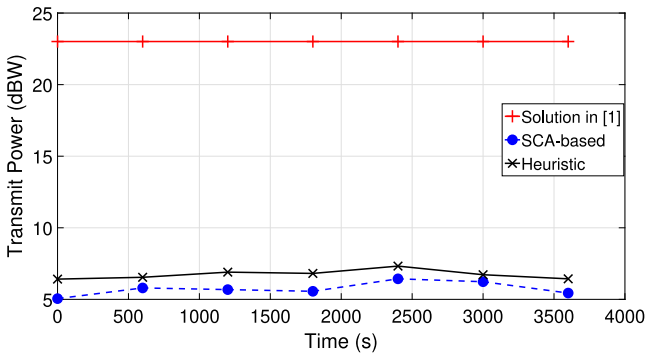

Fig. 7. A comparison of the proposed SCA and heuristic algorithms with the solution proposed in [1] in terms of the satellite transmit power over an orbital period for the case of **low** user demand.

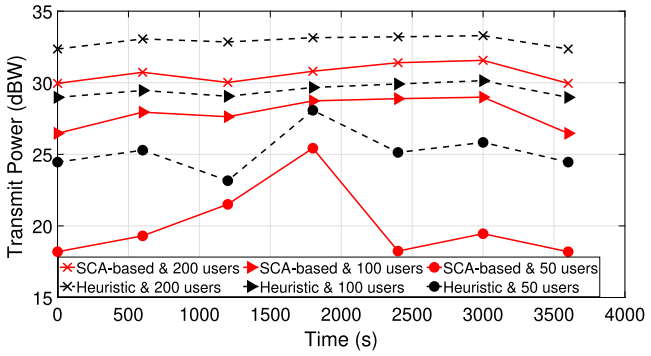

Fig. 8. The satellite transmit power over an orbital period for both the SCA-based and heuristic algorithms, considering different numbers of users, *i.e.,* Scenario-2.

different numbers of users, *i.e.,* Scenario-2. As anticipated, the transmit power required to meet the demand increases with a higher number of users, reflecting the greater capacity needed. Consistent with the previous findings, the SCA-based algorithm consistently outperforms the heuristic algorithm in terms of transmit power efficiency. This observation further supports the superiority of the SCA-based approach in optimizing resource allocation and satisfying user demands in an energy-efficient manner.

6.2. Energy efficiency

We consider energy efficiency (EE), measured in bits-per-Joule, to evaluate the performance of the proposed solutions EE is a widely used and important indicator for communication systems. Let $R_n(t)$ and $P^n_{tot}(t)$ be the total throughput or data rate (bits/sec) and total power (transmission + fixed circuit power) consumed (Watts) of nth LEO satellite in time slot t, respectively. Then EE (b/J) of the satellite network per time slot is defined as follows [44]:

$$EE = \frac{\sum_{n=1}^{N} R_n(t)}{\sum_{n=1}^{N} P^n_{tot}(t)}. \tag{20}$$

Fig. 9 showcases the energy efficiency trends over an orbital period for the proposed heuristic and SCA based algorithms for the high, medium, and low demand cases with a fixed number of users, namely the Scenario-1. Obviously, the SCA-based algorithm outperforms the heuristic algorithm across all demand scenarios. Particularly, in the case of high user demand, the performance gap between the two approaches becomes more pronounced, highlighting the superiority and effectiveness of the SCA-based algorithm over the heuristic approach. This advantage is a result of the SCA-based algorithm's capacity to

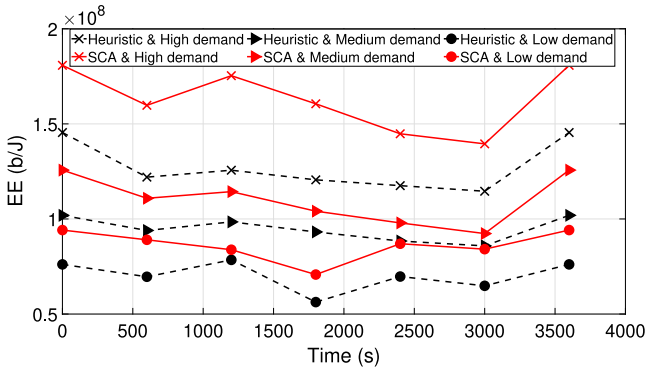

Fig. 9. Energy efficiency performance of the SCA and heuristic algorithms over an orbital period considering different demand cases with a fixed number of users.

Table 2
Performance evaluation of SCA based proposed algorithm.

Avg Demand	Total Power Consumption	Active Satellites	EE (Gb/J)
High	2015.73 W	57%	0.181
Medium	1194.14 W	38%	0.151
Low	512.44 W	28%	0.124

Table 3
Performance evaluation of the proposed heuristic algorithm.

Avg Demand	Total Power Consumption	Active Satellites	EE (Gb/J)
High	2710.95 W	52%	0.134
Medium	1434.36 W	36%	0.126
Low	725.74 W	26%	0.09

find the optimal solution for minimizing power consumption while efficiently meeting the heightened user demands.

The performance evaluation results of the SCA-based and heuristic algorithms are presented in Tables 2 and 3, respectively, for Scenario-2, i.e., varying the number of users. Consistent with Scenario-1 experiment, the results demonstrate the superior performance of the proposed SCA-based algorithm compared to the heuristic algorithm. Additionally, it is observed that as the system demand increases, the number of active satellites, power consumption, and system energy efficiency also increase, which aligns with our intuitive expectations. Evidently, our proposed strategy and developed solutions have led to a substantial improvement in total energy efficiency for LEO satellite communications. Thus, these approaches offer telecommunication companies and satellite operators practical and tangible benefits, ranging from cost savings to improved sustainability, ultimately contributing to the optimization of satellite communication systems and services.

In closing, the proposed technique in this work could significantly enhance energy efficiency in satellite networks, leading to more sustainable and efficient satellite communication systems. However, it is important to mention that this technique relies on a well-structured ground network with enough satellite visibility for effective coordination. Accurate time synchronization is also essential to maintain seamless data transfer between satellites and user terminals. Additionally, propagation delay in LEO satellite networks varies based on satellite separation and transmission paths, with approximately 13.3 ms added for each additional 1000 km in distance [43]. These limitations are essential to consider when implementing the proposed technique, as they may affect the network performance and the feasibility of real-time applications.

7. Conclusions

In this paper, we have proposed a dynamic traffic-aware satellite switch-off approach aimed at minimizing power consumption in LEO satellite constellations. Our approach takes into account the heterogeneous distribution of users in terms of time and location, as well as the relative motion of satellites. By strategically shutting down satellite nodes during low demand periods and over unpopulated regions, we aim to reduce overall power consumption without compromising user demands. To this end, a mixed binary integer optimization problem has been formulated. An iterative SCA based and a slant distance based heuristic algorithms were proposed to solve the formulated optimization problem without causing any demand dissatisfaction. Through extensive simulations utilizing practical constellation patterns and realistic traffic demands obtained from a maritime dataset, we evaluated the performance of our developed algorithms. Further, performance comparisons are provided to demonstrate the validity and gains of the proposed solutions over the solution provided in [1]. The results have shown that a considerable percentage of the satellite nodes can be dispensable and switched-off, leading to substantial energy savings. In short, our proposed approaches have the potential to significantly reduce energy consumption in satellite constellations, making them promising solutions for achieving sustainability and efficiency in satellite communication systems.

CRediT authorship contribution statement

Vaibhav Kumar Gupta: Writing – original draft, Validation, Software, Methodology, Formal analysis. **Hayder Al-Hraishawi:** Writing – review & editing, Validation, Investigation. **Eva Lagunas:** Writing – review & editing, Supervision, Resources, Project administration, Methodology, Investigation, Funding acquisition, Conceptualization. **Symeon Chatzinotas:** Writing – review & editing, Supervision, Resources, Project administration, Funding acquisition.

Declaration of competing interest

The authors declare the following financial interests/personal relationships which may be considered as potential competing interests: Eva Lagunas reports financial support was provided by Luxembourg National Research Fund (FNR). If there are other authors, they declare that they have no known competing financial interests or personal relationships that could have appeared to influence the work reported in this paper.

Appendix. Proof of Theorem 1

The sketch of the proof consists of similar procedure as the related proofs in [31], [32]. Herein, we demonstrate the equivalence of problems (9) and (11). To this end, let first consider the optimal solution of problem (9) is $\mathbf{Z}^*$. The Lagrangian function of problem (9) is expressed as $\mathcal{L}(\mathbf{P},\mathbf{X},\mathbf{Y},\alpha_1,\alpha_2) =$

$$\sum_{n=1}^{N}\sum_{m=1}^{M} P_{n,m} + \sum_{n=1}^{N} P_c\ Y_n + \alpha_1(G_x(\mathbf{X}) - F_x(\mathbf{X})) + \alpha_2(G_y(\mathbf{Y}) - F_y(\mathbf{Y})), \quad \text{(A.1)}$$

where α_1 and α_2 are the Lagrange multipliers corresponding to the constraints C8b and C8d, respectively. Also, recall that $G_x(\mathbf{X}) - F_x(\mathbf{X}) \geq 0$ and $G_y(\mathbf{Y}) - F_y(\mathbf{Y}) \geq 0$. Now, we obtain the following inequality[7] from Lagrange duality [35]:

$$\mathbf{Z}_d^* = \max_{\alpha_1,\alpha_2\geq 0}\ \min_{\mathbf{P},\mathbf{X},\mathbf{Y}\in\Omega} \mathcal{L}(\mathbf{P},\mathbf{X},\mathbf{Y},\alpha_1,\alpha_2) \quad \text{(A.2)}$$

[7] Recall that weak duality holds for convex and non-convex optimization problems [35].

$$\overset{(a)}{\leq} \min_{\mathbf{P},\mathbf{X},\mathbf{Y}\in\Omega} \max_{\alpha_1,\alpha_2\geq 0} \mathcal{L}(\mathbf{P},\mathbf{X},\mathbf{Y},\alpha_1,\alpha_2) = \mathbf{Z}^*, \tag{A.3}$$

where Ω is the set of feasible solutions of problem (9). Now, we will first establish the strong duality. Suppose $(\mathbf{P}^*,\mathbf{X}^*,\mathbf{Y}^*,\alpha_1^*,\alpha_2^*)$ is the solution of the problem (A.2). Further, the following two cases are possible.

Case 1: $G_x(\mathbf{X}) - F_x(\mathbf{X}) > 0$ and $G_y(\mathbf{Y}) - F_y(\mathbf{Y}) > 0$

The optimal value of both the α_1^* and α_2^* is infinite. Hence, $\mathbf{Z}_d^*$ is also infinite which contradicts the fact that it is upper bounded by $\mathbf{Z}^*$.

Case 2: $G_x(\mathbf{X}) - F_x(\mathbf{X}) = 0$ and $G_y(\mathbf{Y}) - F_y(\mathbf{Y}) = 0$

Then both the problems (A.2) and (A.3) are identical since both are independent of α_1^* and α_2^*. Hence, $\mathbf{Z}_d^* = \mathbf{Z}^*$. Strong duality is therefore established, and we can concentrate on addressing the dual problem (A.2) rather than the primary problem (A.3).

Further, we demonstrate that any $\alpha_1 > \alpha_{1,0}$, and $\alpha_2 > \alpha_{2,0}$, where $\alpha_{1,0}$ and $\alpha_{2,0}$ are sufficiently large numbers, are optimal solutions for the dual problem (A.2). We prove this by showing that the following function is monotonic increasing function of α_1 and α_2

$$\overset{\Delta}{=} \min_{\mathbf{P},\mathbf{X},\mathbf{Y}\in\Omega} \mathcal{L}(\mathbf{P},\mathbf{X},\mathbf{Y},\alpha_1,\alpha_2). \tag{A.4}$$

Note that $G_x(\mathbf{X}) - F_x(\mathbf{X}) \geq 0$ and $G_y(\mathbf{Y}) - F_y(\mathbf{Y}) \geq 0$ always hold for any $(\mathbf{P},\mathbf{X},\mathbf{Y},\alpha_1,\alpha_2) \in \Omega$.

Therefore, $\mathcal{L}(\mathbf{P},\mathbf{X},\mathbf{Y},\alpha_1(1),\alpha_2(1)) \leq \mathcal{L}(\mathbf{P},\mathbf{X},\mathbf{Y},\alpha_1(2),\alpha_2(2))$ for $0 \leq \alpha_1(1) \leq \alpha_1(2)$, $0 \leq \alpha_2(1) \leq \alpha_2(2)$ and any $(\mathbf{P},\mathbf{X},\mathbf{Y}) \in \Omega$. This implies $\Phi(\alpha_1(1),\alpha_2(1)) \leq \Phi(\alpha_1(2),\alpha_2(2))$ and proves that $\Phi(\alpha_1,\alpha_2)$ is a monotonic increasing function of α_1 and α_2. This result leads to the fact that $\Phi(\alpha_1,\alpha_2) = \mathbf{Z}^*$ $\forall \alpha_1 > \alpha_{1,0}$, and $\alpha_2 > \alpha_{2,0}$.

In conclusion, strong duality allows us to use the dual problem (A.2) to solve the primal problem (A.3) and any $\alpha_1 > \alpha_{1,0}$, and $\alpha_2 > \alpha_{2,0}$ are ideal dual variables. This completes the proof. □

Data availability

No data was used for the research described in the article.

References

[1] V.K. Gupta, H. Al-Hraishawi, E. Lagunas, S. Chatzinotas, Traffic-aware satellite switch-off technique for LEO constellations, in: IEEE Globel Commun. (Globecom) Workshops, 2022, pp. 880–885, http://dx.doi.org/10.1109/GCWkshps56602.2022.10008660.

[2] R. Deng, B. Di, H. Zhang, L. Kuang, L. Song, Ultra-dense LEO satellite constellations: How many LEO satellites do we need? IEEE Trans. Wirel. Commun. 20 (8) (2021) 4843–4857, http://dx.doi.org/10.1109/TWC.2021.3062658.

[3] H. Al-Hraishawi, H. Chougrani, S. Kisseleff, E. Lagunas, S. Chatzinotas, A survey on non-geostationary satellite systems: The communication perspective, IEEE Commun. Surv. Tuts. 25 (1) (2023) 101–132, http://dx.doi.org/10.1109/COMST.2022.3197695.

[4] X. Lin, S. Rommer, S. Euler, E.A. Yavuz, R.S. Karlsson, 5G from space: An overview of 3GPP non-terrestrial networks, IEEE Commun. Stand. Mag. (2021).

[5] T. Heyn, A. Hofmann, S. Raghunandan, L. Raschkowski, Non-terrestrial networks in 6G, in: Shaping Future 6G Networks: Needs, Impacts, and Technologies, John Wiley & Sons, 2022, pp. 101–116, http://dx.doi.org/10.1002/9781119765554.ch8.

[6] J.A. Fraire, G. Nies, C. Gerstacker, H. Hermanns, K. Bay, M. Bisgaard, Battery-aware contact plan design for LEO satellite constellations: The ulloriaq case study, IEEE Trans. Green Commun. Netw. 4 (1) (2020) 236–245, http://dx.doi.org/10.1109/TGCN.2019.2954166.

[7] H. Al-Hraishawi, S. Chatzinotas, B. Ottersten, Broadband non-geostationary satellite communication systems: Research challenges and key opportunities, in: IEEE Int. Conf on Commun Workshops, ICC Workshops, Montreal, QC, Canada, 2021, pp. 1–6.

[8] V.S. Borkar, S. Choudhary, V.K. Gupta, G.S. Kasbekar, Scheduling in wireless networks with spatial reuse of spectrum as restless bandits, Perform. Eval. (ISSN: 0166-5316) 149–150 (2021) 102208, http://dx.doi.org/10.1016/j.peva.2021.102208.

[9] M.N. Dazhi, H. Al-Hraishawi, B. Shankar, S. Chatzinotas, B. Ottersten, Energy-efficient service-aware multi-connectivity scheduler for uplink multi-layer non-terrestrial networks, IEEE Trans. Green Commun. Netw. (2023) 1–14, http://dx.doi.org/10.1109/TGCN.2023.3269283.

[10] R. Surampudi, J. Blosiu, P. Stella, J. Elliott, J. Castillo, T. Yi, J. Lyons, M. Piszczor, J. McNatt, C. Taylor, et al., Solar power technologies for future planetary science missions, Jet Propuls. Lab Calif. Inst. Technol. (2017).

[11] F. Leverone, M. Pini, A. Cervone, E. Gill, Solar energy harvesting on-board small satellites, Renew. Energy (ISSN: 0960-1481) 159 (2020) 954–972, http://dx.doi.org/10.1016/j.renene.2020.05.176.

[12] ETSI TR 103 352 V1.1.1, Satellite Earth Stations and Systems (SES); Energy Efficiency of Satellite Broadband Network, Technical Report, ETSI, Sophia Antipolis Cedex-France, 2016.

[13] H. Tsuchida, Y. Kawamoto, N. Kato, K. Kaneko, S. Tani, S. Uchida, H. Aruga, Efficient power control for satellite-Borne batteries using Q-learning in low-earth-orbit satellite constellations, IEEE Wirel. Commun. Lett. 9 (6) (2020) 809–812, http://dx.doi.org/10.1109/LWC.2020.2970711.

[14] J. Hu, G. Li, D. Bian, L. Gou, C. Wang, Optimal power control for cognitive LEO constellation with terrestrial networks, IEEE Commun. Lett. 24 (3) (2020) 622–625, http://dx.doi.org/10.1109/LCOMM.2019.2961880.

[15] H. Tsuchida, Y. Kawamoto, N. Kato, K. Kaneko, S. Tani, M. Hangai, H. Aruga, Improvement of battery lifetime based on communication resource control in low-earth-orbit satellite constellations, IEEE Trans. Emerg. Top. Comput. 10 (3) (2022) 1388–1398, http://dx.doi.org/10.1109/TETC.2021.3087489.

[16] Q. Liao, M. Kaneko, Global energy efficiency optimization of a Ka-band multi-beam LEO satellite communication system, IEEE Access 9 (2021) 55232–55243, http://dx.doi.org/10.1109/ACCESS.2021.3071475.

[17] V.K. Gupta, V.N. Ha, E. Lagunas, H. Al-Hraishawi, L. Chen, S. Chatzinotas, Combining time-flexible GEO satellite payload with precoding: The cluster hopping approach, IEEE Trans. Veh. Technol. (2023) 1–15, http://dx.doi.org/10.1109/TVT.2023.3292554.

[18] H. Al-Hraishawi, M. Minardi, H. Chougrani, O. Kodheli, J.F.M. Montoya, S. Chatzinotas, Multi-layer space information networks: Access design and soft-warization, IEEE Access 9 (2021) 158587–158598, http://dx.doi.org/10.1109/ACCESS.2021.3131030.

[19] S. Liu, J. Lin, L. Xu, X. Gao, L. Liu, L. Jiang, A dynamic beam shut off algorithm for LEO multibeam satellite constellation network, IEEE Wirel. Commun. Lett. 9 (10) (2020) 1730–1733.

[20] Z. Tang, C. Wu, Z. Feng, B. Zhao, W. Yu, Improving availability through energy-saving optimization in LEO satellite networks, in: Inf. and Commun. Technol. EurAsia Conf., Springer, 2014, pp. 680–689.

[21] M. Hussein, A. Abu-Issa, I. Tumar, A. Awad, Reducing power consumption in LEO satellite network, Int. J. Elect. Comput. Eng. 11 (3) (2021) 2256.

[22] H. Al-Hraishawi, J. ur Rehman, S. Chatzinotas, Quantum optimization algorithm for LEO satellite communications based on cell-free massive MIMO, in: IEEE Int. Conf on Commun. (ICC) Workshops, 2023, pp. 1–6.

[23] V.M. Baeza, E. Lagunas, H. Al-Hraishawi, S. Chatzinotas, An overview of channel models for NGSO satellites, in: IEEE Veh. Technol. Conf. (VTC2022-Fall), London, United Kingdom, 2022, pp. 1–6, http://dx.doi.org/10.1109/VTC2022-Fall57202.2022.10012693.

[24] 3GPP TR 38.811V15.1.0, 3rd Generation Partnership Project; Technical Specification Group Radio Access Network; Study on New Radio (NR) to Support Non Terrestrial Networks (Release 15), Technical Report, 3rd Generation Partnership Project, 2019.

[25] 3GPP TR 38.821, 3rd Generation Partnership Project; Technical Specification Group Radio Access Network; Solutions for NR to Support Non-Terrestrial Networks (NTN) (Release 16), Technical Report, 3rd Generation Partnership Project, 2019.

[26] A. Guidotti, A. Vanelli-Coralli, A. Mengali, S. Cioni, Non-terrestrial networks: Link budget analysis, in: IEEE Int. Conf on Commun. (ICC), 2020, pp. 1–7, http://dx.doi.org/10.1109/ICC40277.2020.9149179.

[27] A. Adhikary, J. Nam, J.-Y. Ahn, G. Caire, Joint spatial division and multiplexing—The large-scale array regime, IEEE Trans. Inform. Theory 59 (10) (2013) 6441–6463, http://dx.doi.org/10.1109/TIT.2013.2269476.

[28] R. Wang, M.A. Kishk, M.-S. Alouini, Ultra-dense LEO satellite-based communication systems: A novel modeling technique, IEEE Commun. Mag. 60 (4) (2022) 25–31, http://dx.doi.org/10.1109/MCOM.001.2100800.

[29] A. Al-Hourani, An analytic approach for modeling the coverage performance of dense satellite networks, IEEE Wirel. Commun. Lett. 10 (4) (2021) 897–901, http://dx.doi.org/10.1109/LWC.2021.3049179.

[30] J. Tang, D. Bian, G. Li, J. Hu, J. Cheng, Resource allocation for LEO beam-hopping satellites in a spectrum sharing scenario, IEEE Access 9 (2021) 56468–56478, http://dx.doi.org/10.1109/ACCESS.2021.3072059.

[31] D.W.K. Ng, Y. Wu, R. Schober, Power efficient resource allocation for full-duplex radio distributed antenna networks, IEEE Trans. Wirel. Commun. 15 (4) (2016) 2896–2911, http://dx.doi.org/10.1109/TWC.2015.2512919.

[32] Y. Sun, D.W.K. Ng, Z. Ding, R. Schober, Optimal joint power and subcarrier allocation for full-duplex multicarrier non-orthogonal multiple access systems, IEEE Trans. Commun. 65 (3) (2017) 1077–1091, http://dx.doi.org/10.1109/TCOMM.2017.2650992.

[33] M. Grant, S. Boyd, CVX: Matlab software for disciplined convex programming, version 2.2, 2014, http://cvxr.com/cvx.

[34] T. Lipp, S.P. Boyd, Variations and extension of the convex–concave procedure, Optim. Eng. 17 (2016) 263–287.

[35] S. Boyd, L. Vandenberghe, Convex Optimization, Cambridge University Press, 2004, http://dx.doi.org/10.1017/CBO9780511804441.
[36] J.G. Walker, Satellite constellations, J. Br. Interplanet. Soc. 37 (1984) 559–572.
[37] I. Leyva-Mayorga, B. Soret, M. R00F6per, D. W00FCbben, B. Matthiesen, A. Dekorsy, P. Popovski, LEO small-satellite constellations for 5G and beyond-5G communications, IEEE Access 8 (2020) 184955–184964, http://dx.doi.org/10.1109/ACCESS.2020.3029620.
[38] J. Galtier, Real-time resource allocation for LEO satellite constellations, Wirel. Netw. 15 (6) (2009) 791–803.
[39] S. Cakaj, The parameters comparison of the starlink LEO satellites constellation for different orbital shells, Front. Commun. Netw. 2 (2021) 643095.
[40] H. Al-Hraishawi, E. Lagunas, S. Chatzinotas, Traffic simulator for multibeam satellite communication systems, in: 10th Advanced Satellite Multimedia Syst. Conf. and the 16th Signal Process. for Space Commun. Workshop, ASMS/SPSC, 2020, pp. 1–8.
[41] C. Lu, J. Shi, B. Li, X. Chen, Dynamic resource allocation for low earth orbit satellite networks, Phys. Commun. (ISSN: 1874-4907) 67 (2024) 102498, http://dx.doi.org/10.1016/j.phycom.2024.102498.
[42] H. Tsuchida, Y. Kawamoto, N. Kato, K. Kaneko, S. Tani, S. Uchida, H. Aruga, Efficient power control for satellite-Borne batteries using Q-learning in low-earth-orbit satellite constellations, IEEE Wirel. Commun. Lett. 9 (6) (2020) 809–812, http://dx.doi.org/10.1109/LWC.2020.2970711.
[43] X. Li, X. Zhang, J. Chang, Dynamic low earth orbit multi satellite hopping beam resource allocation considering load and dynamic coverage balance (LDCB-MSHBRA), Discov. Space 128 (2024) http://dx.doi.org/10.1007/s11038-024-09557-5.
[44] F. Liu, K. Zheng, W. Xiang, H. Zhao, Design and performance analysis of an energy-efficient uplink carrier aggregation scheme, IEEE J. Sel. Areas Commun. 32 (2) (2014) 197–207, http://dx.doi.org/10.1109/JSAC.2014.141202.